ELSEVIER

Journal of Quantitative Spectroscopy & Radiative Transfer 109 (2008) 1834–1844

Journal of Quantitative Spectroscopy & Radiative Transfer

www.elsevier.com/locate/jqsrt

Water vapor line width and shift calculations with accurate vibration–rotation wave functions

A.D. Bykov[a], N.N. Lavrentieva[a], T.P. Mishina[a], L.N. Sinitsa[a,*], R.J. Barber[b], R.N. Tolchenov[b], J. Tennyson[b]

[a]*The Institute of Atmospheric Optics, Av. Akademicheskii 1, 634055 Tomsk, Russian Federation*
[b]*Department of Physics and Astronomy, University College London, Gower Street, WC1E 6BT London, UK*

Received 11 July 2007; received in revised form 8 January 2008; accepted 9 January 2008

Abstract

Calculations of $H_2^{16}O$ rotation–vibration line broadening and shifting due to N_2 pressure effects are performed using a semi-empirical approach. The calculations are based on impact theory modified by introducing additional parameters to extend the use of empirical data. These model parameters are determined by fitting the broadening and shifting coefficients to experimental data. The method is further developed by using anharmonic wavefunctions in the estimates of the line profiles. The main feature of the present calculation is the use of a complete set of high-accuracy vibration–rotation dipole transition moments calculated for all possible transitions using wavefunctions determined from variational nuclear motion calculations and an *ab initio* dipole moment surface. This approach explicitly takes into account all scattering channels induced by collisions. Results of these calculations clearly demonstrate improved agreement between observed and calculated parameters for both the line widths and the line shifts.
© 2008 Elsevier Ltd. All rights reserved.

Keywords: Contour of spectral line; Line width and shift coefficients; Semi-classical impact theory

1. Introduction

An accurate knowledge of the water vapor line pressure broadening and shifting coefficients induced by N_2, O_2 and other atmospheric gases is of interest for many atmospheric applications including models of the propagation of laser radiation along vertical and slanted paths [1]. Consequently, there have been a large number of line parameter measurements spanning a wide spectral region, from the microwave to the visible [2–11]. Indeed, the line broadening and shifting behavior of rotation–vibration spectra are important for many water vapor radiation transmittance problems, both at room temperature and for excited media, which makes their characterization a subject of considerable recent interest. The availability of a large number of accurate measurements of water vapor line parameters in the microwave, infrared and visible spectral regions makes the water problem a benchmark one for testing theories of spectral pressure effects. Accurate calculations of

*Corresponding author. Tel.: +7 3822 491527; fax: +7 3822 492086.
E-mail addresses: lnn@iao.ru, sln@iao.ru (L.N. Sinitsa).

0022-4073/$ - see front matter © 2008 Elsevier Ltd. All rights reserved.
doi:10.1016/j.jqsrt.2008.01.006

water vapor half-widths and line center shifts require improvement to semi-classical RB theory [12]; see for instance [13–16], which is the main method of calculation at the present time. Apart from refining the general formulae of the theory, calculations require accurate wave functions, energy levels and collision-induced transition probabilities. It should be noted that most previous studies [17–22] have used wave functions determined from simple models of intra-molecular motion based on effective Hamiltonians.

There are two important reasons as to why a correct treatment of intra-molecular motion is necessary. Firstly, when calculating line contour parameters, the transitions between low-lying vibrational states that do not have large-amplitude vibrational modes, such as inversion or torsion, it is only necessary to correct for anharmonicity, Coriolis coupling or centrifugal distortion. In the case of low-lying states these are normally minor adjustments since the vibrational amplitudes are usually small in comparison to the equilibrium distances between the atoms. However, for transitions to highly excited states, the intra-molecular motion cannot be treated as small-amplitude vibrations, and as a consequence, corrections due to the intra-molecular interactions are usually large and cannot be reliably determined by a perturbative approach. Therefore one needs to use more accurate wave functions than those given by effective Hamiltonians.

Secondly, the energy level density for highly excited ro-vibrational states is great, which means that there are numerous interactions, such as Fermi, Coriolis or Darling–Dennison resonances, between different vibrational states. Consequently the zero-order wave functions are strongly mixed and it is necessary to take into account many additional transitions when calculating widths and shifts. It is not possible to use simple transition strength rules based on approximate quantum numbers, such as the asymmetric top quantum numbers K_a and K_c, and vibrational quantum numbers v_1, v_2 and v_3. In addition to their energies, the only quantum numbers that can be used for highly excited states are the angular momentum and symmetry.

In this article we estimate the influence of the intra-molecular effects on line width and shift using the near exact ro-vibrational wave functions calculated using the variational approach. The paper is organized as follows. Section 2 contains a description of BT2 line list. In Section 3 a brief outline of the theoretical background and details of the contour parameters calculations are presented. In Section 4 the results of our calculations and their comparison with experimental data are discussed.

2. DVR3D and the BT2 line list

A number of procedures [23–25] are available for calculating the rotation–vibration spectra of triatomic molecules, such as water, by direct solution of the Schrödinger equation. These procedures have been shown to be capable of achieving experimental accuracy [26], and for water the accuracy of such calculations is determined by the quality of the available potential energy surface that must include allowances for the failure of the Born–Oppenheimer approximation [27]. A number of high-accuracy *ab initio* [27–29] and semi-empirical [28,30,31] potential energy surfaces are available for water. Variational nuclear motion calculations on such surfaces yield energy levels and associated nuclear motion wave functions. In this work we also require dipole transition moments that can be obtained using appropriate dipole moment surfaces (DMS). The best available DMS are ones calculated *ab initio* [32,33] and here we use the one due to Schwenke and Partridge [32].

In this work we use energy levels and dipole transition moments from the BT2 line list [34]. This line list was constructed using the DVR3D nuclear motion suite [25], the semi-empirical PES of Shirin et al. [30] and Schwenke and Partridge's DMS [32]. The BT2 line list includes all transitions between rotation–vibration states of water up to 30,000 cm^{-1} above the ground state and with rotational excitation up to $J = 50$. This gives a total of 221,000 states, which cover a larger range than is required for the present study. The BT2 line list gives dipole intensities for all rigorously allowed transitions without resource to rules given by approximate quantum numbers. It contains a total of 5.08×10^8 transitions. Further information can be found in the original publication [34].

3. Method and calculation

To calculate the pressure broadening and shifting coefficients of the H_2O spectral lines due to various gases, we use a semi-empirical technique that incorporates corrections to the ATC (Anderson–Tsao–Curnutte)

method [35,36]. This approach works within the framework of the impact approximation. The general assumptions in this case are as follows: collisions are considered as binary, the duration of a collision is less than the time between collisions, the translational motions of particles are treated using a classical paths approximation, and no line mixing effects occur. Full details of the semi-empirical approach are described in Ref. [37]; a short description is presented below.

According to the general formulation of the semi-classical theory, the half-width γ_{if} and the line center shift δ_{if} associated with the transition $i \to f$ can be written as

$$\gamma_{fi} + i\delta_{fi} = \frac{n}{c}\sum_{p}\rho(p)\int_0^\infty vf(v)\,\mathrm{d}v\int_0^\infty bU(i,f,p,b,v)\,\mathrm{d}b. \tag{1}$$

The efficiency function $U(i,f,p,b,v)$ is

$$\begin{aligned}\mathrm{Re}\,U(i,f,p,b,v) = 1 - \left\{1 - S^{(L)}_{2,fp,ip}\right\}\cos\left[S_{1,fp} - S_{1,ip} + \mathrm{Im}\,S_{2,fp} - \mathrm{Im}\,S_{2,ip}\right] \\ \times \exp\left[-\left(\mathrm{Re}\,S_{2,fp} + \mathrm{Re}\,S_{2,ip} + S^{(C)}_{2,fp,ip}\right)\right],\end{aligned} \tag{2}$$

$$\begin{aligned}\mathrm{Im}\,U(i,f,p,b,v) = \left\{1 - S^{(L)}_{2,fp,ip}\right\}\sin\left[S_{1,fp} - S_{1,ip} + \mathrm{Im}\,S_{2,fp} - \mathrm{Im}\,S_{2,ip}\right] \\ \times \exp\left[-\left(\mathrm{Re}\,S_{2,fp} + \mathrm{Re}\,S_{2,ip} + S^{(C)}_{2,fp,ip}\right)\right],\end{aligned}$$

where n is the density of perturbing particles, $\rho(p)$ is the thermal population of level p, p is the set of quantum numbers of perturbing particles, v is the relative collision velocity, $f(v)$ is the Maxwell velocity distribution function, b is the impact parameter, S_1 and S_2 are the usual first- and second-order terms of the ATC theory, and the indices (L) and (C) represent the efficiency functions associated with "linked" and "connected" diagrams of the perturbation theory. S_1 is defined by the isotropic part in the inter-molecular potential and S_2 is defined by its anisotropic part. Both parts depend on the trajectory of relative motion. Eqs. (1) and (2) represent the general formulation of the semi-classical theory and they should be expanded to include the relative trajectory of the colliding particles, the inter-molecular potential at both short and long separations, and simultaneous consideration of adiabatic and non-adiabatic effects associated with the S_1 and S_2 terms.

Expressions (1) and (2) depend on dipole transition strengths $D^2(ii'|l)$ and $D^2(ff'|l)$ of different scattering channels $i \to i'$, $f \to f'$ connecting lower and upper levels of a transition with other closely spaced levels. These parameters are square reduced matrix elements of the molecular constants, such as components of the dipole vector or components of the quadrupole tensor. The contour parameters of the Anderson theory can be expressed as

$$\gamma_{if} = A(i,f) + \sum_{i'} D^2(ii'|l)P_l(\omega_{ii'}) + \sum_{f'} D^2(ff'|l)P_l(\omega_{ff'}) + \cdots \tag{3}$$

and

$$\delta_{if} = B(i,f) + \sum_{i'} D^2(ii'|l)P_l(\omega_{ii'}) + \sum_{f'} D^2(ff'|l)P_l(\omega_{ff'}) + \cdots$$

neglecting higher-order terms. Here

$$P_l(\omega) = \frac{n}{c}\sum_{p}\rho(p)\sum_{l',p'}A_{ll'}D^2(pp'|l')F_{ll'}\left(\frac{2\pi c b_0(p,i,f)}{v}(\omega + \omega_{pp'})\right) \tag{4}$$

is the efficiency function for the scattering channel $i \to i'$ or $f \to f'$ (if the frequencies $\omega_{ii'}$ and $\omega_{ff'}$ are substituted instead of ω). The term

$$A(i,f) = \frac{n}{c}\sum_{p}\rho(p)\int_0^\infty vF(v)b_0^2(v,p,i,f)\,\mathrm{d}v$$

is the usual term of ATC theory due to integral cut-off ($b_0(v,p,i,f)$ is the cut-off parameter);

$$B(i,f) = \frac{n}{c} B_1 \left\{ \alpha_2(\mu_f^2 - \mu_i^2) + 3\varepsilon\varepsilon_2(\alpha_f - \alpha_i)/[2(\varepsilon + \varepsilon_2)] \right\} \sum_p \rho(p) \int_0^\infty vF(v) b_0^{-3}(v,p,i,f)\,\mathrm{d}v$$

is the contribution of the isotropic part of the potential, α, μ and ε are the polarizability, dipole moment and ionization potential of the H_2O molecule, respectively, α_2 and ε_2 are the polarizability and ionization potential of the perturbing molecule, $B_1 = -3\pi/(8\hbar v)$. The $A_{ll'}$'s are the parameters for the particular ll'-type interaction. Terms with $l = 1$ correspond to dipole transitions and those with $l = 2$ correspond to quadrupole transitions in the radiative molecule.

The transition strengths $D^2(ii'|l)$ and $D^2(ff'|l)$ related to the scattering channels $i \to i'$, $f \to f'$ depend only on the radiative properties of the molecule (dipole or quadrupole moments) and therefore only depend on intra-molecular effects. They may have different characteristics, resulting from electrostatic or atom–atom components of the inter-molecular potential. The expansion coefficients $P_l(\omega_{ii'})$ depend on the properties of the absorbing molecule; they depend on the inter-molecular potential, trajectory, energy levels and wave functions of the buffer molecule. As proposed in [37] the efficiency functions $P_l(\omega)$ can be represented as

$$P_l(\omega) = P_l^A(\omega) C_l(\omega), \tag{5}$$

where $P_l^A(\omega)$ is the efficiency function of ATC theory and $C_l(\omega)$ is a correction factor, which is determined from fitting to experimental data. The function $P_l^A(\omega)$ remains the most important term in the calculation: it determines all the main contributions to the broadening; the factor $C_l(\omega)$ gives only a small correction connected with trajectory curvature, short-range forces or higher-order terms in the perturbation expansion of scattering matrix.

The H_2O–N_2 calculations were performed with the correction factor taken simply as a j-dependent efficiency function:

$$P_l(\omega_{ff'}) = P_l^A(\omega_{ff'}) \left[c_1 \Big/ \left(c_2 \sqrt{j_f + 1} \right) \right], \tag{6}$$

where c_1 and c_2 are fitting parameters. The form of the correction factor for $P_l(\omega_{ii'})$ is similar to expression (6), only with index f replaced by i.

The calculation requires molecular constants for H_2O: mean dipole moments in the ground and excited vibrational states were taken from [38], components of quadrupole moments from [39] and the dipole polarizability from [40]. The H_2O–N_2 calculations were performed with c_1 [H_2O–N_2] = 1.08 and c_2

Table 1
"Effective" dipole polarizability in the upper vibrational states

Band	Polarizability (Å^3)
v_2	1.496
v_3	1.502
v_1	1.510
$v_1 + v_2 + v_3$	1.561
$v_1 + 2v_3$	1.606
$2v_1 + v_3$	1.572
$2v_1 + 2v_2 + v_3$	1.601
$3v_1 + v_3$	1.609
$v_1 + 3v_3$	1.660
$3v_1 + v_2 + v_3$	1.631
$3v_1 + 2v_2 + v_3$	1.640
$4v_1 + v_3$	1.641
$4v_1 + v_2 + v_3$	1.646
$5v_1 + v_3$	1.655
$5v_1 + v_2 + v_3$	1.690
$6v_1 + v_3$	1.682
$7v_1 + v_3$	1.710

$[H_2O–N_2] = 0.11$. We used one more fitted parameter for the line shift calculation—the "effective" dipole polarizability in the upper vibrational state; these are listed in Table 1.

4. Results and discussion

Prior to the current work, the semi-empirical method presented above and the effective Hamiltonian (EH) approach were used for calculations of line contour parameters and their temperature exponents for $H_2O–N_2$, $H_2O–O_2$, $CO_2–N_2$ and $CO_2–O_2$ colliding systems [20,21,41]. The results of these calculations have been included in a freely available carbon dioxide spectroscopic data bank [42] and in the "ATMOS" Information System [43].

In this paper, the semi-empirical method is expanded and accurate variational wave functions are used to calculate the width and shift coefficients of water vapor lines induced by N_2 pressure. The use of the accurate wave functions resulting from extensive variational nuclear motion calculations produces an improvement in width and shift parameters and, in principle, extends the range of applicability of the method up to dissociation [44]. It should be stressed that such massive calculations are not possible within the EH method, since EH parameters—rotational, centrifugal distortion and resonance coupling constants—are usually determined from experimental spectra. The other obstacle preventing the use of the EH method, which is based on perturbation theory expansions, for transitions in the visible and near UV spectra is its poor convergence for highly excited states. Variational methods do not suffer from these problems and, in principle, take account of all intra-molecular effects.

In the case of the $H_2O–N_2$ collisions, the main contribution to the pressure broadening and shifting is due to interaction between the dipole moment of water and the quadrupole moment of N_2. We have also taken into account the higher-order electrostatic terms: quadrupole–quadrupole, as well as the induction and dispersion terms of the polarization potential. The contribution of quadrupole–quadrupole interactions (which is less than 5%) was taken into account using a Watson Hamiltonian approach. Some of the BT2 levels do not have full quantum number assignments (that is, no quantum numbers in normal modes notation); these levels are mostly associated with weak lines. In this case it is not possible to include quadrupole–quadrupole interactions.

The use of our cut procedure is valid for molecules characterized by strong interactions, when the distance of closest approach is less than the interruption parameter, i.e. $r_c > b_0$ where r_c is the distance of closest approach and b_0 is the interception radius. The N_2 molecule has no dipole moment but enough big quadrupole moment (-1.4×10^{-26} esu [45]), so $r_c > b_0$ for most transitions for the $H_2O–N_2$ colliding system. The influence of short-range forces is small in this case and is taken into account by the correction factor.

To take account of the dipole transitions caused by inter-molecular interaction we use the dipole transition probabilities $D^2(ii'|l)$ and $D^2(ff'|l)$ derived from the Einstein A coefficients in BT2, which are used for the line intensity calculation. It was necessary to select the required Einstein A coefficients from the 500 million values presented in the full BT2 list. We estimated the contributions of corresponding scattering channels to the line contour parameters and then sorted the Einstein A coefficients. In the calculation of line broadening and shift parameters, we took account of all the scattering channels induced by collisions and allowed by symmetry; many more than in the standard Watson Hamiltonian approach. It was found that contributions from scattering channels with $\omega_{ii'} > 700\,\mathrm{cm}^{-1}$ and $K_a - K_a' > 3$ are negligible.

We have performed numerous test calculations to make a detailed analysis of the factors determining a variety of line shift and broadening coefficients. The calculations of broadening and shift coefficient of the water lines induced by N_2 were performed for ro-vibrational bands covering a wide spectral range from the mid-IR to the visible (with vibrational quantum number up to 7), see Table 2. All calculations were for a temperature $T = 297\,\mathrm{K}$. The parameters c_1 and c_2 were fitted to the measured N_2-broadening coefficients of the $2v_1 + 2v_2 + v_3$ band and were used for all subsequent calculations of both N_2-broadening and shifting.

Our calculated values were compared both with experimental data and with calculations performed using the Watson effective Hamiltonian (see Table 3 and Figs. 1–3). Table 3 contains the results of calculations using both methods for the $7v_2$ band. Spectroscopic EH parameters for the (0 7 0) state were taken from [46]. It can be seen that half-widths calculated using variational wave functions agree reasonably well with those obtained using the standard approach of perturbative wave functions from Watson's effective Hamiltonian and an

Table 2
Water vapor bands studied in this work

N	Band	N	Band	N	Band	N	Band
1	$7v_1+v_3$	11	$6v_2+3v_3$	21	$3v_1+2v_2+v_3$	31	$2v_1+2v_2+v_3$
2	$5v_1+2v_2+v_3$	12	$3v_1+4v_2+v_3$	22	$v_1+v_2+3v_3$	32	$v_1+4v_2+v_3$
3	$6v_1+v_3$	13	$2v_1+v_2+3v_3$	23	$3v_2+3v_3$	33	$3v_3$
4	$4v_1+3v_2+v_3$	14	$v_1+3v_2+3v_3$	24	$3v_1+v_2+v_3$	34	$2v_3$
5	$v_1+v_2+5v_3$	15	$4v_1+v_2+v_3$	25	$2v_1+3v_2+v_3$	35	v_3
6	$5v_1+v_2+v_3$	16	$5v_2+3v_3$	26	$v_1+5v_2+v_3$	36	
7	$3v_1+3v_3$	17	$3v_1+3v_2+v_3$	27	v_1+3v_3	37	
8	$2v_1+2v_2+3v_3$	18	$2v_1+3v_3$	28	$2v_2+3v_3$	38	
9	$4v_1+2v_2+1v_3$	19	$v_1+2v_2+3v_3$	29	$7v_2+v_3$	39	
10	$5v_1+v_3$	20	$4v_2+3v_3$	30	$3v_1+v_3$	40	

All bands start from the ground vibrational state.

Table 3
Line parameters for the $7v_2$ band: calculated by two methods: (a) using wave functions from a Watson effective Hamiltonian; (b) using variational wave functions (BT2)

f	i	Shift (a)	Shift (b)	Halfwidth (a)	Halfwidth (b)
827	936	−0.013	−0.020	0.092	0.083
615	744	−0.030	−0.038	0.068	0.067
726	835	−0.013	−0.015	0.091	0.090
845	954	−0.034	−0.044	0.063	0.063
854	963	−0.035	−0.049	0.053	0.046
853	964	−0.034	−0.048	0.053	0.045
844	955	−0.034	−0.030	0.058	0.063
735	844	−0.026	−0.026	0.077	0.078
753	862	−0.036	−0.051	0.051	0.044
752	863	−0.035	−0.052	0.052	0.044
744	853	−0.034	−0.044	0.060	0.058
743	854	−0.033	−0.045	0.058	0.052
625	734	−0.013	−0.015	0.090	0.089
835	946	−0.029	−0.036	0.062	0.060
826	937	−0.015	−0.026	0.060	0.057
909	918	−0.014	−0.022	0.062	0.069
808	817	−0.013	−0.020	0.073	0.074
845	936	−0.021	−0.018	0.083	0.083
918	927	−0.022	−0.016	0.081	0.070
734	827	−0.020	−0.025	0.058	0.056
717	624	−0.018	−0.015	0.095	0.095

effective dipole moment operator. For most lines the differences in half-widths do not exceed 10%. However, the differences are larger for shift coefficients usually about 20% but up to 35% in some cases. This demonstrates that the shift coefficients are more sensitive to different intra-molecular interactions.

As previously mentioned, the density of the ro-vibrational states in the high-energy region results in strong mixing between zero-order wave functions. This mixing cannot be accounted for within simple EH calculations when resonances are neglected (isolated vibrational state approximation, see, for instance, Refs. [16,18,20,21]). Moreover, at the moment there are no EH parameters for polyads above 16,000 cm^{-1}. Even in the case of low-lying resonance polyads, one needs to takes into account many additional transitions that can be strong due to wave function mixing. Such contributions were ignored when determining the collision scattering-matrix elements in all previous line width and shift calculations [16,18,20,21]. This means that the differences between calculations made by the two methods should correlate with values of mixing coefficients for the vibration states involved in resonances.

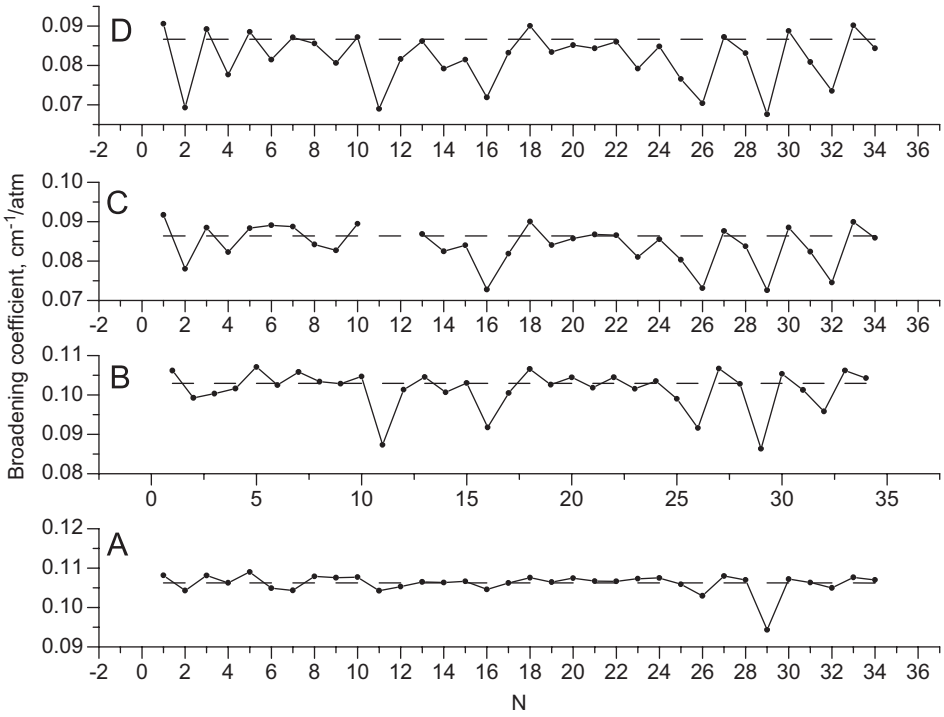

Fig. 1. Broadening coefficients for the (A) $4_{04} \leftarrow 3_{03}$, (B) $2_{20} \leftarrow 2_{21}$, (C) $5_{32} \leftarrow 4_{32}$ and (D) $4_{31} \leftarrow 3_{30}$ transitions as functions of band numbers N from Table 3. Dashed lines correspond to γ calculated using the Watson Hamiltonian approach.

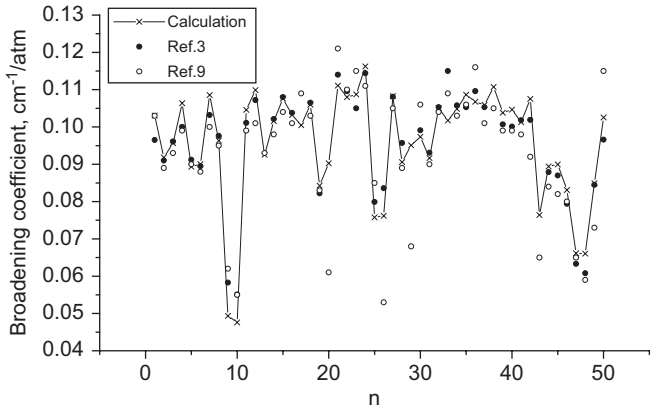

Fig. 2. Comparison of calculated and measured broadening coefficients for lines of the $3\nu_1 + \nu_3$ band. Line numbers correspond to the numbering given in Ref. [41].

Fig. 1 shows broadening coefficients calculated using BT2 wave functions for the $4_{04} \leftarrow 3_{03}$ (Fig. 1A), $2_{20} \leftarrow 2_{21}$ (Fig. 1B), $5_{32} \leftarrow 4_{32}$ (Fig. 1C) and $4_{31} \leftarrow 3_{30}$ (Fig. 1D) transitions for 35 bands whose numbering corresponds to that presented in Table 2. Dashed lines show the results of a calculation made using a Watson's effective Hamiltonian approach for low-lying bands. For the $4_{04} \leftarrow 3_{03}$ transitions, the two calculations result in coefficients that are practically the same for all bands. However, the situation for the $4_{31} \leftarrow 3_{30}$ transitions is very different; calculations without any vibrational dependence give a coefficient of $0.087\,\mathrm{cm^{-1}\,atm^{-1}}$ but calculations that use BT2 coefficients vary from 0.066 to $0.091\,\mathrm{cm^{-1}\,atm^{-1}}$. The largest discrepancies are for the high-lying $5\nu_1 + 2\nu_2 + \nu_3$ ($0.069\,\mathrm{cm^{-1}\,atm^{-1}}$), $6\nu_2 + 3\nu_3$ ($0.069\,\mathrm{cm^{-1}\,atm^{-1}}$) and $7\nu_2 + \nu_3$ ($0.066\,\mathrm{cm^{-1}\,atm^{-1}}$).

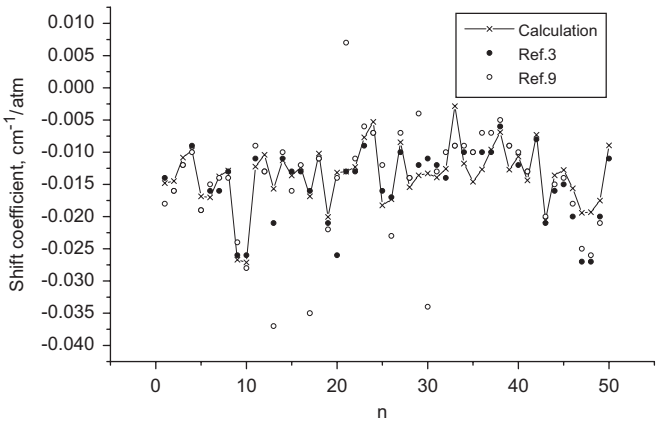

Fig. 3. Comparison of calculated and measured shifting coefficients for lines of the $3\nu_1+\nu_3$ band. Line numbers correspond to the numbering given in Ref. [41].

The discrepancies increase dramatically with higher rotational quantum numbers and the differences can be positive or negative. For example, the discrepancy in the broadening coefficient of transitions where seven quanta of bending vibration is excited ($7\nu_2+\nu_3$ band), $\Delta\gamma$ reaches 27% for the $8_{26}\leftarrow 7_{07}$ line.

Fig. 1 clearly demonstrates the correlation between broadening coefficients in different bands in the high-frequency range. Transitions in the bands involving highly excited bending states have broadening coefficients significantly smaller than average. The decreasing line width in these bands is influenced by centrifugal distortion—the so-called Δk effect [47], which leads to a strong change in the energy structure in high bending states.

Recent theoretical and experimental studies show that in the high-frequency region vibrational amplitudes are large and it is necessary to take into account vibrational dependence of the broadening coefficients. However a recent Franco-Belgian experimental study [9,10] made using a Fourier transform spectrometer derived broadening coefficients in the 13,000–26,000 cm^{-1} range, which differ dramatically from those presented in the HITRAN database. The largest broadening values obtained by these studies, which are in the 0.4–1 $cm^{-1}\,atm^{-1}$ range, are more than three times bigger than the highest values given in spectroscopic databases.

To understand this problem, we have compared our numerous calculations on almost 40 bands with two extended experimental studies of high-frequency water lines broadened by nitrogen: (1) the previously mentioned study [9,10], which considered H_2O lines broadened by N_2 and H_2O using Fourier transform spectrometer in the 13,000–26,000 cm^{-1} range and (2) the measurements by Grossman and Browell [3] who considered line broadening and shifting for the $3\nu_1+\nu_3$ and $2\nu_1+2\nu_2+\nu_3$ water vapor bands measured with a diode laser spectrometer in the 13,558–13,965 cm^{-1} region with spectral resolution of 0.0001 cm^{-1}. In this last experiment the broadening coefficients vary from 0.051 to 0.115 $cm^{-1}\,atm^{-1}$.

In Fig. 2 we compare our calculated γ-values with the experimental ones for the $3\nu_1+\nu_3$ band for the lines that were measured in both experiments. The figure shows that the experiments [3,9,10] differ strongly. The discrepancies between the measurements reach 0.02 $cm^{-1}\,atm^{-1}$ (25%). Our calculations agree well with the experimental values of [3], with a root mean square (RMS) of 0.0056 $cm^{-1}\,atm^{-1}$, and poorly with the FTS experiment [9] (RMS = 0.011 $cm^{-1}\,atm^{-1}$ for the same lines).

It should be noted that the calculated broadening coefficients in the 37 bands we have examined do not exceed 0.15 $cm^{-1}\,atm^{-1}$. Analysis of the spectral intervals where [9,10] give large broadening coefficients shows that they are characterized by blended lines. For example:

The line at 18,816.25 cm^{-1} with $\gamma = 0.414\,cm^{-1}\,atm^{-1}$ ($2_{12}\leftarrow 1_{10}$ of the $\nu_1+3\nu_2+3\nu_3$ band) overlaps with the line at 18,816.17 cm^{-1} ($2_{21}\leftarrow 1_{10}$ of the $2\nu_1+\nu_2+3\nu_3$ band).

The line at 18,850.97 cm^{-1} with $\gamma = 0.407\,cm^{-1}\,atm^{-1}$ consists of an unresolved doublet, $5_{50}\leftarrow 5_{51}$ and $5_{51}\leftarrow 5_{50}$ of the $\nu_1+3\nu_2+3\nu_3$ band.

The line at 19,445.64 cm^{-1} with $\gamma = 0.502\,cm^{-1}\,atm^{-1}$ is a doublet: ($6_{42} \leftarrow 7_{61}$ from the $4\nu_1 + 2\nu_2 + \nu_3$ band and ($6_{43} \leftarrow 7_{62}$ from the $3\nu_1 + 4\nu_2 + \nu_3$ band).

For such cases the fitting of a single profile to blended lines leads to very significant overestimation of the broadening. To correct this problem, it is necessary to undertake a thorough analysis and assignment of the

Table 4
Root mean square deviation of calculated halfwidths from available experimental data in the 10,000–23,000 cm^{-1} range

Spectral band $(v_1,v_2,v_3)^{up}-(v_1,v_2,v_3)_{low}$	$(Halfwidth)_{RMS}$	Spectral band $(v_1,v_2,v_3)^{up}-(v_1,v_2,v_3)_{low}$	$(Halfwidth)_{RMS}$
[50]		[9]	
All bands	0.0051	103–000	0.0286
003–000	0.0061	104–000	0.1114
022–000	0.0007	113–010	0.1043
102–000	0.0067	113–000	0.0820
121–000	0.0043	122–000	0.0418
201–000	0.0047	123–000	0.0531
220–000	0.0033	133–000	0.3496
300–000	0.0056	141–000	0.0434
[51]		142–000	0.0272
All bands	0.0087	151–000	0.0791
221–000	0.0134	160–000	0.0348
301–000	0.0058	202–000	0.0310
[52]		203–000	0.0453
All bands	0.0049	212–000	0.0533
121–000	0.0031	213–000	0.0552
201–000	0.0046	221–000	0.0237
300–000	0.0058	222–000	0.0690
[3]		223–000	0.0841
All bands	0.0036	231–000	0.0352
202–000	0.0030	240–000	0.0465
221–000	0.0041	241–000	0.0569
301–000	0.0033	301–000	0.0269
[53]		302–000	0.0426
All bands	0.0072	303–000	0.0707
003–000	0.0053	311–010	0.0995
102–000	0.0081	311–000	0.0300
121–000	0.0049	320–000	0.0461
201–000	0.0081	321–000	0.0231
300–000	0.0096	330–000	0.0483
221–000	0.0070	331–000	0.0053
103–000	0.0084	340–000	0.0673
301–000	0.0066	341–000	0.1364
113–000	0.0103	400–000	0.0346
311–000	0.0097	401–000	0.0502
[9]		402–000	0.0563
All bands	0.0639	410–000	0.0277
004–000	0.0448	411–000	0.1117
023–000	0.0415	420–000	0.0535
033–000	0.0462	500–000	0.0338
042–000	0.0359	501–000	0.0279
043–000	0.0593	510–000	0.0350
053–000	0.0512	511–000	0.0613
061–000	0.0342	600–000	0.0352
063–000	0.7747	601–000	0.0463
071–000	0.0072	700–000	0.0473

spectrum, which was subsequently done in Ref. [48], and then use this as a basis for a reparameterization of the line contours in the measured spectra, which is yet to be done.

For the line shifting coefficients, δ, the situation is similar, see Fig. 3. Comparison of the calculated δ-values with the experimental ones for the $3\nu_1+\nu_3$ band also demonstrates that experiments [3,9,10] again differ from each other very strongly. Sometimes the shift coefficients of [9,10] are more than double those of [3], or even differ in sign. The experimental data of [3] agree very well with our calculations (RMS = 0.00056 cm^{-1} atm^{-1}). The agreement of experimental data [9,10] with our calculations is much worse (RMS = 0.0009 cm^{-1} atm^{-1}).

We find that the largest disagreement between BT2 and EH calculations takes place for high bending vibration. The present calculated broadening and shifting coefficients agree well with those calculated previously using a complex version of Robert–Bonamy theory (CRBF) [49] for the $3\nu_1+\nu_3$ band. This band involves no excitation of bending vibrations and the EH method works well; RMS are the same for calculations using EH or variational wavefunctions. Conversely, for the $2\nu_1+2\nu_2+\nu_3$ band, which involves two quanta of bending excitation, our method gives better agreement with the experimental data [3]. For example, the RMS of line shifts is 0.0005 cm^{-1} atm^{-1} for CRBF calculations [49] and 0.0004 cm^{-1} atm^{-1} for our calculations.

After testing our computational procedure against experimental data, we made calculations using this method for more than 200,000 transitions, corresponding to the most intense lines, for the H_2O–N_2 colliding systems. Line broadening and shifting coefficients, as well as their temperature exponents, have been calculated. The results of these calculations are available via the "ATMOS" Information System (http://saga.atmos.iao.ru).

Calculated line widths were compared with experimental values from [3,9,47,50–54] in diapason of 10,000–23,000 cm^{-1}. RMS for different experiments and different bands are presented in the tables. Lines for which the experimental assignment differs strongly from BT2 assignment were removed from the comparison (Table 4).

Line broadening parameters for more than 4000 lines of 35 bands in the region above 10,000 cm^{-1} were included in the comparison. It should be emphasized that our calculations use only two fitting parameters. Analysis of the data presented in the tables shows that these calculations are in good agreement with experimental data.

Acknowledgments

The authors acknowledge the support by RAS Program "Optical Spectroscopy and Frequency Standards", NERC, the Royal Society and INTAS Grant no. 03-51-3394.

References

[1] Zuev VV, Ponomarev YN, Solodov AM, Tikhomirov BA, Romanovsky OA. Opt Lett 1985;10:318–20.
[2] Grossman BE, Browell EV. J Mol Spectrosc 1989;136:264–94.
[3] Grossman BE, Browell EV. J Mol Spectrosc 1989;138:562–95.
[4] Chevillard J-P, Mandin J-Y, Flaud J-M, Camy-Peyret C. Can J Phys 1991;69:1286–98.
[5] Yamada KMT, Harter M, Giesen T. J Mol Spectrosc 1993;157:84–94.
[6] Tobin DC, Strow LL, Lafferty WJ, Olson WB. Appl Opt 1996;35:4724–34.
[7] Toth RA. J Mol Spectrosc 2000;201:218–43.
[8] Rinsland CP, Goldman A, Smith MA, Devi VM. Appl Opt 1991;30:1427–38.
[9] Coheur P-F, Fally S, Carleer M, Clerbaux C, Colin R, et al. JQSRT 2002;749:493–510.
[10] Coheur P-F, Fally S, Carleer M, Clerbaux C, Colin R, et al. JQSRT 2003;82:119–31.
[11] Gamache RR, Hartmann J-M. Can J Chem 2004;82:1013–27.
[12] Robert D, Bonamy JJ. J Phys 1979;40:923–43.
[13] Bykov AD, Lavrent'eva NN, Sinitsa LN. Atmos Oceanic Opt 1992;5:587–94.
[14] Buldyreva J, Bonamy JJ, Robert D. JQSRT 1999;62:321–43.
[15] Buldyreva J, Benec'h S, Chrysos M. Phys Rev A 2000;63:012708.
[16] Lavrent'eva NN, Starikov VI. Mol Phys 2006;112:1932–9.
[17] Lynch R, Gamache RR, Neshyba SP. J Chem Phys 1996;105:5711–21.
[18] Bykov A, Lavrent'eva N, Sinitsa L. Opt Spektrosk 1997;83:73–82.

[19] Gamache RR, Lynch R, Plateaux JJ, Barbe A. JQSRT 1997;57:485–96.
[20] Valentin A, Claveau Ch, Bykov A, Lavrentieva N, Saveliev V, Sinitsa L. J Mol Spectrosc 1999;198:218–29.
[21] Zéninari V, Parvitte B, Courtois D, Lavrentieva NN, Ponomarev YuN, Durry G. Mol Phys 2004;102:1697–706.
[22] Camy-Peyret C, Valentin A, Claveau Ch, Bykov A, Lavrentieva N, Saveliev V, et al. J Mol Spectrosc 2004;224:164–75.
[23] Tennyson J, Miller S, Le Sueur CR. Comput Phys Commun 1993;75:339.
[24] Schwenke DW. Comput Phys Commun 1992;70:1.
[25] Tennyson J, Kostin MA, Barletta P, Harris GJ, Ramanalal J, Polyansky OL, et al. Comput Phys Commun 2004;163:85.
[26] Polyansky OL, Tennyson J. J Chem Phys 1999;110:5056.
[27] Polyansky OL, Csaszar AG, Shirin SV, Zobov NF, Barletta P, Tennyson J, et al. Science 2003;299:539.
[28] Partridge H, Schwenke DW. J Chem Phys 1997;106:4168.
[29] Barletta P, Shirin SV, Zobov NF, Polyansky OL, Tennyson J, Valeev EF, et al. J Chem Phys 2006;125:204307.
[30] Shirin SV, Polyansky OL, Zobov NF, Barletta P, Tennyson J. J Chem Phys 2003;118:2124.
[31] Shirin SV, Polyansky OL, Zobov NF, Ovsyannikov RI, Csaszar AG, Tennyson J. J Mol Spectrosc 2006;236:216.
[32] Schwenke DW, Partridge H. J Chem Phys 2003;113:6592.
[33] Lodi L, Tolchenov RN, Tennyson J, Lynas-Gray A-E, Shirin SV, Zobov NF, et al. , J Chem Phys 2008;128:044304.
[34] Barber RJ, Tennyson J, Harris GJ, Tolchenov RN. Mon Not R Astron Soc 2006;368:1087–94.
[35] Anderson PW. Phys Rev 1949;76:657–61.
[36] Tsao CJ, Curnutte B. JQSRT 1962;2:41–91.
[37] Bykov A, Lavrent'eva N, Sinitsa L. Mol Phys 2004;102:1706–12.
[38] Shostak SL, Muenter JS. J Chem Phys 1991;94:5883.
[39] Flygare WH, Benson RC. Mol Phys 1971;20:225.
[40] Murphy WF. J Chem Phys 1977;67:5877.
[41] Tashkun SA, Perevalov VI, Teffo J-L, Bykov AD, Lavrentieva NN. CDSD-1000. JQSRT 2003;82:165–96.
[42] 〈ftp://ftp.iao.ru/pub/CDSD-1000〉.
[43] 〈http://saga.atmos.iao.ru〉.
[44] Mussa HY, Tennyson J. J Chem Phys 1998;109:10885–92.
[45] Mulder F, Van Dijk G, Van der Avoird A. Mol Phys 1980;39:407–25.
[46] Bykov AD, Voronin BA, Voronina SS. Atmos Oceanic Opt 2002;15:953–7.
[47] Bykov AD, Makushkin YUS, Stroinova VN. Opt Spektrosk 1988;64:517–20.
[48] Tolchenov RN, Zobov NF, Shirin SV, Polyansky OL, Tennyson J, Naumenko O, et al. J Mol Spectrosc 2005;233:68–76.
[49] Lynch R, Gamache RR, Neshyba SP. JQSRT 1998;59:595–613.
[50] Mandin JY, Chevillard JP, Camy-Peyret C, Flaud JM. J Mol Spectrosc 1989;138:272–81.
[51] Wilkerson TD, Schwemmer G, Gentry B, Giver LP. JQSRT 1979;22:315–31.
[52] Giver LP, Gentry B, Schwemmer G, Wilkerson TD. JQSRT 1982;27:423–36.
[53] Mandin JY, Chevillard JP, Flaud JM, Camy-Peyret C. J Mol Spectrosc 1989;138:430–9.
[54] 〈http://faculty.uml.edu/Robert_Gamache〉.